Journal of
Molecular
Modeling

FULL PAPER

Three-Dimension Quantitative Structure-Activity Relationship Analysis of Some Cinnamamides Using Comparative Molecular Similarity Indices Analysis (CoMSIA)

Tingjun Hou, Youyong Li, Ning Liao, and Xiaojie Xu

College of Chemistry and Molecular Engineering, Peking University, Beijing 100871, P. R. China.
E-mail: xiaojxu@chemms.chem.pku.edu.cn

Abstract Comparative molecular similarity indices analysis (CoMSIA) has been applied to a data set of cinnamamides. Five different properties: steric, electrostatic, hydrophobic, H-bond donor and H-bond acceptor, assumed to cover the major contributions to ligand binding, were used to generate the 3D-QSAR model. A significant cross-validated correlation coefficient q^2 (0.691) was obtained, indicating the statistical significance of the model for untested compounds of this class. The model was used to predict the anticonvulsant activities of five test-set compounds, and the predicted values were in good agreement with the experimental results. Moreover, from the contour maps, the key features vital to ligand binding have been identified, which are important for us to trace the important properties and gain insight into the potential mechanisms of intermolecular interactions between ligand and receptor.

Keywords CoMSIA, Cinnamamides, CoMFA, 3D-QSAR

Introduction

The cinnamamide analogues have received much attention because they possess a wide spectrum of physiological functions [1-3], including nervous suppression, hypnosis, sedation, anticonvulsion, muscular relaxation, local anesthesia and mycostate. Among this class of compounds, 3,4-(Methylenedioxy)cinnamoyl piperidide, simplified to poperine II, has been regarded as a potential anti-epilepsy drug [4] for its inherent anticonvulsant activity. Clinical use shows that this compound actually has relatively good therapeutic effectiveness for different epileptic patients and rela-

tively few untoward effects. The basic structure of 3,4-(methylenedioxy)cinnamoyl piperidide (Chart 1) is a vinyl group (B region), with a hydrophobic benzene ring on one end (A region) and an amido group (C region) on the other. Previous studies have shown that the benzene ring of part A
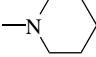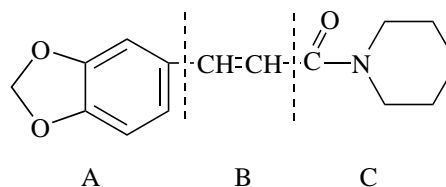

Chart 1 *Structure of 3,4-(methylenedioxy)cinnamoyl piperidide*

Correspondence to: X. Xu

Table 1 *Structures of cinnamamide derivatives [a] and experimental and calculated biological activity by the 3D-QSAR model from CoMSIA(1) in Table 2*

No.	-R	X	log(1/C) obsd.	log(1/C) calcd.	Residue
1 [b]	—N⟨ ⟩ (cycloamine)	3-Cl	0.788	0.615	0.173
2		3-F	0.578	0.500	0.078
3		4-F	0.458	0.501	-0.043
4		4-Br	0.314	0.442	-0.128
5		2,4-Cl	0.664	0.651	0.013
6		3,4-Cl	0.550	0.647	-0.097
7		4-Cl	0.606	0.514	0.092
8 [b]		4-NO$_2$	0.268	0.344	-0.076
9		3-NO$_2$	0.324	0.323	0.001
10		3-CF$_3$	0.921	0.897	0.023
11		2-CF$_3$	0.723	0.699	0.021
12		4-CF$_3$	0.921	0.881	0.039
13		3-OH, 4-OCH$_3$	-0.272	-0.330	0.060
14		4-OCH$_3$	0.218	0.185	0.035
15		3-I	0.320	0.406	-0.086
16 [b]		4-OC$_2$H$_5$	0.500	0.442	0.058
17		4-OC$_3$H$_7$-n	0.290	0.257	0.033
18		4-OC$_4$H$_9$-n	0.180	0.242	-0.062
19		3-Cl	0.410	0.555	-0.145
20		3-F	0.495	0.562	-0.072
21		4-F	0.495	0.506	-0.016
22		4-Br	0.540	0.523	0.017
23	–NHC$_4$H$_9$-i	2,4-Cl$_2$	0.735	0.705	0.025
24 [b]		3,4-Cl$_2$	0.977	0.722	0.255
25		4-Cl	0.714	0.540	0.170
26		4-CF$_3$	0.772	0.849	-0.079
27		3-CF$_3$	0.989	0.890	0.099
28		3-Cl	0.620	0.501	0.119
29		4-F	0.288	0.464	-0.174
30		4-Br	0.580	0.472	0.108
31	–NHC$_3$H$_7$-i	2,4-Cl$_2$	0.600	0.668	-0.068
32 [b]		4-Cl	0.801	0.722	0.079
33		3,4-Cl$_2$	0.498	0.531	-0.031
34		4-CF$_3$	0.899	0.831	0.069
35		3-CF$_3$	0.924	0.901	0.019

[a] See Chart 2
[b] These compounds were used as test set and not included in the derivation of equations

Chart 2 *General structure of the cinnamamide derivatives*
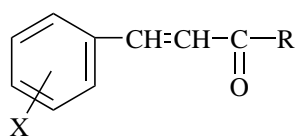
is necessary for the activity. On the benzene ring, the substitution of 4-chloro-, 2-chloro-groups and so on for hydrogen atoms favors the anticonvulsant activity. The -CH=CH- in part B is also critical to the activity. When the double bond is saturated or cut to one carbon atom, the anticonvulsant activity is considerably reduced. The amides composed of the amines of relatively small groups in part C, e.g., isopropyl amine, *sec*-butylamine, and cycloamylamine, show stronger anticonvulsant activity than the others [5].

Until now, however, few studies on the relationship between the chemical structures and the biological functions of the cinnamamide analogues (Chart 2) have been reported. Our early work has established a structure-activity profile for a set of cinnamamide analogues using molecular shape analysis [6] and 2D-QSAR based on a genetic algorithm [7]. Due to the limitations of a single method, the combination of several methods may be important to understand the key features contributing to ligand binding. Here, a newly developed 3D-QSAR procedure: comparative molecular similarity indices analysis (CoMSIA) is used to understand the key factors contributing the ligand binding. With the results of our previous study [6-7], some useful information directly related to the anticonvulsant mechanisms of cinnamamides is expected to be determined.

Computational methods

The principles of CoMSIA

From its advent in 1988, CoMFA has been developed as one of the most powerful tools in 3D-QSAR [8]. CoMFA examines differences in targeted properties which are related to changes in the shape of the non-covalent (steric and electrostatic) fields surrounding a set of ligand molecules. Details of the shape of each field are put into a QSAR table by sampling their magnitudes at regular intervals throughout a specified region of space. Recently, another 3D-QSAR procedure: comparative molecular similarity indices analysis (CoMSIA) has been reported [9]. This method can avoid some inherent deficiencies arising from the functional form of Lennard-Jones and Coulomb potentials used in CoMFA. In CoMSIA, a distance dependent Gaussian-type functional form has been introduced, which can avoid singularities at the atomic positions and the dramatic changes of potential energy for those grids in the proximity of the surface, meanwhile, no arbitrary definition of cut-off limits is required in CoMSIA. Moreover, using CoMSIA, the contour maps of the relative spatial contributions of the different fields can be substantially improved, which is very intuitive for interpretation in terms of separate property fields.

Similar to the conventional CoMFA procedure, the procedure of getting a 3D-QSAR model from a CoMSIA approach can be summarized into three steps below [9-11]:

(1) First, all investigated molecules are structure-based or field-based aligned.

(2) Then, an evenly-spaced and rectangular grid is generated to enclose the molecular aggregate. A probe atom with some properties is placed at every lattice point to measure the electrostatic, steric, hydrophobic, H-bond donor or acceptor field.

(3) Finally, the results from the field samplings combined with the biological activities from the tested compounds are put into a table and partial least squares (PLS) is applied to get the final CoMSIA model.

Generally, a leave-one-out cross-validated r^2 (q^2) will be used as a quantitative measure for a CoMSIA model. The unique difference between conventional CoMFA and CoMSIA is the field type and the potential function. In CoMSIA, the similarity is expressed in terms of different physicochemical properties: steric occupancy, partial atomic charges, local hydrophobicity, and H-bond donor and acceptor properties. A Gaussian-type distance dependent function is used to calculate different kinds of physicochemical properties. The indices $A_{F,K}$ between the compounds of interest and a probe atom have been calculated according to:

$$A_{F,K}^{q}(j) = -\sum_{i=1}^{n} \omega_{probe,k}\, \omega_{ik}\, e^{-\alpha r_{iq}^{2}}$$

where i: summation index over all atoms of the molecule j under investigation; ϖ_{ik}: actual value of the physicochemical

property k of atom, $\varpi_{probe,\,k}$: probe atom with charge +1, radius 1 Å, hydrophobicity +1, H-bond donor and acceptor property +1; a: attenuation factor; r_{iq}: mutual distance between probe atom at grid point q and atom i of the investigated molecule.

Data set and structure alignment

35 cinnamamide analogs were synthesized (Table 1) [12]. The chemical structures of these compounds were all modified from 3,4 – methylendioxy-cinnamoyl piperidide at several sites. These compounds were tested on mice for anticonvulsant activity through the maximal electroshock seizures test (MES), the value of ED_{50} could be calculated by using the Weil method [12]. The potency was defined as $\log(1/C)$ (C represents ED_{50}) in the QSAR analysis and used as a dependent variable in the QSAR study (Table 1). A training set of 30 cinnamamides was used for CoMSIA analyses. In addition, 5 compounds, selected from various ranges of anticonvulsant activity, were kept to test the actual prediction of the model.

The molecular geometries of all compounds in Table 1 were modeled using the SYBYL molecular simulation package [13]. The initial structures were first minimized using molecular mechanics with the MMFF94 force field [14]. Then those structures were fully optimized, and Mulliken charges were calculated based on the semiempirical AM1 method [15], available in MOPAC 7.0 [16]. From the 3D structures, it can be found that the series of compounds possess relatively rigid core structures constituting a large conjugated system. So a rigid alignment was applied to superimpose all 35 compounds onto an unsubstituted template shown in Chart 2 using an atom-by-atom least-square fit as implemented in the SYBYL FIT option, and compound 27 with the best biological activity as the reference molecule. In Chart 3, the six carbon atoms of benzene ring in the A region, the atoms in
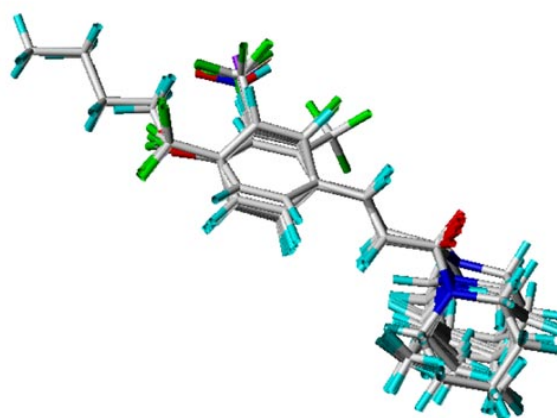

Figure 1 *Plot of all aligned compounds in the training and test set*

Table 2 *Results of the different CoMSIA analyses for the training data set: (1) three field with 2 Å grid spacing; (2) five fields with 1.5 Å grid spacing; (3) five fields with 1.0 Å grid spacing*

	CoMSIA(1)	CoMSIA(2)	CoMSIA(3)
q^2	0.691	0.687	0.687
r^2	0.888	0.910	0.910
Standard error of estimate	0.098	0.090	0.090
F	49.538	48.591	48.612
No. comp	4	5	5
Fraction			
steric	0.060	0.076	0.078
electrostatic	0.376	0.392	0.397
hydrophobic	0.266	0.236	0.214
H-donor	0.209	0.170	0.126
H-acceptor	0.089	0.120	0.158
grid spacing (Å)	2.0	1.5	1.0

Chart 3 *The template structure used as fit centers*
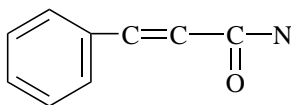
the B region and the amido group in C region were selected as the fit centers. Figure 1 shows the aligned molecules (including the test set) within the grid box (grid spacing 2.0 Å) used to generated the CoMSIA columns.

Determination of the 3D-QSAR models

In the present CoMSIA analyses, five kinds of physicochemical properties, including steric contributions by the third power of the atomic radii, electrostatics by atomic AM1 Mulliken charges, hydrophobicities by atom-based hydrophobic parameters and hydrogen-bonding properties by suitably placed pseudoatoms, have been evaluated, using a common probe with 1 Å radius, +1 charge, +1 hydrophobicity and H-bond property of +1. The value of the attenuation factor *a* was defined as 0.3. A lattice of 2 Å was generated to surround the whole molecular aggregates after the alignment. The surrounding lattice was selected with a sufficiently large margin (= 4 Å) to enclose all aligned molecules. The effect of grid point spacing on the CoMSIA analysis was also investigated at 1.5 and 1 Å with the same orientation (Table 2).

To choose the appropriate components and check the statistical significance of the models, leave-one-out cross-validations were used by the enhanced version of PLS, the SAMPLES method. Then the final 3D-QSAR model was derived from the no cross-validation calculations. The CoMSIA results were graphically interpreted by field contribution maps using the field type "stdev*coeff".

As a comparison, a conventional CoMFA was performed with the usually used steric and electrostatic fields in SYBYL. The AM1 Mulliken charges were applied in the determination of the electrostatic field. All CoMFA calculations were performed with the SYBYL standard setup (steric and elec-

trostatic fields with Lennard-Jones and Coulomb-type potentials, dielectric constant 1/r, cutoff 30 kcal mol^{-1}) using an sp^3 carbon atom with a charge of +1.0 |e|. The extent and the orientation of the grids surrounding the tested molecules were as the same as those in CoMSIA analysis, and the grid spacing was set to 2 Å. All calculations in this study were performed in SYBYL on an SGI R10000 workstation.

Results and discussion

Predictive power of the 3D-QSAR model

The final results of the CoMSIA analyses with 2.0, 1.5 and 1.0 Å grid spacing are shown in Table 2. Although all three PLS analyses yielded similar and consistent results, the model with 2.0 Å is selected as the best model judged by the cross-
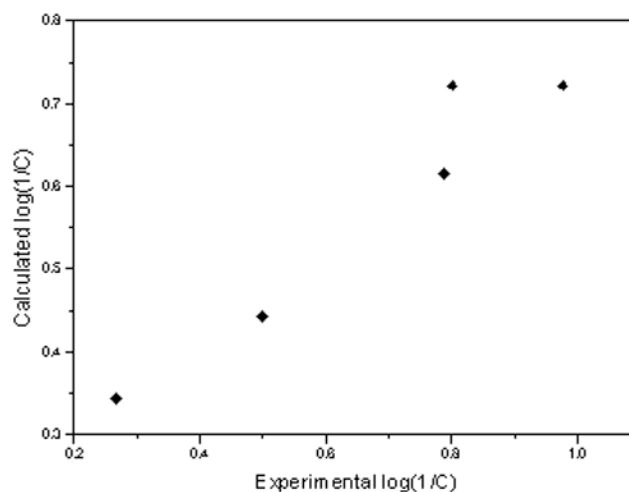
Figure 2 *Comparison of experimental log(1/C) with calculated log(1/C) obtained using the 3D-QSAR model from CoMSIA(1)*

Table 3 *Results of the CoMSIA analyses of several different field combinations with 2.0 Å grid spacing*

	CoMFA	steric + electrostatic	electrostatic + hydrophobic	electrostatic + hydrophobic + H-bonding
q^2	0.198	0.318	0.601	0.587
r^2	0.462	0.770	0.836	0.884
Standard error of estimate	0.202	0.140	0.140	0.102
F	24.864	20.879	44.127	36.445
No. comp	1	4	3	5
Fraction				
steric	0.489	0.170		
electrostatic	0.511	0.830	0.554	0.408
hydrophobic			0.446	0.335
H-donor				0.257
H-acceptor				

validated correlation, and the following discussions will only refer to the model generated from 2.0 Å grid spacing. The optimal components that produce the best cross-validation linear regression coefficient were used to produce the non-cross-validated model. The leave-one-out cross-validated PLS analysis results in a q^2 of 0.691 using five principle components, and the non-cross-validated PLS analysis yields a higher r^2 of 0.888 with a low standard error of estimate (SD) 0.098. The anticonvulsant activity (log1/C), the calculated activities using the 3D-QSAR model from CoMSIA(1), and the residue values for training set are shown in Table 1. Figure 2 shows the plot of observed *vs* calculated anticonvulsant activity. The predicted biological activities of the five molecules in the test set are also listed in Table 1, and the best 3D-QSAR model has a good prediction for the five tested com-
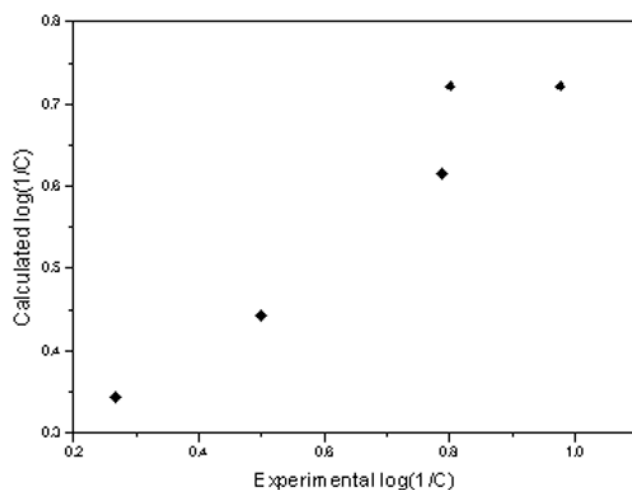
Figure 3 *Plot of the actual prediction of 3D-QSAR from CoMSIA(1) for five test compounds*

pounds (Figure 3). So the derived model was satisfactory in respect of statistical significance and actual predictive ability. On the basis of the best 3D-QSAR model obtained, we expect to find more potential compounds with the aid of the computational combinatorial chemistry method.

Table 3 shows the analysis results from CoMFA and several sets of analysis results of different field combinations from CoMSIA. Only using the steric and electrostatic fields, the 3D-QSAR model from CoMSIA analysis does not have good statistical significance ($q^2 = 0.318$). Meanwhile, that model from CoMFA is also dissatisfactory. So it can be concluded that the biological activity can not be well expressed by only using the steric and electrostatic fields. After addition of the hydrophobic field, the predictive power of the 3D-QSAR model ($q^2 = 0.601$) is increased significantly, indicating that there essentially exists a significant relationship between the biological activity and the hydrophobic field. It seems that the entropic contribution to binding affinity cannot be considered completely by only using steric and electrostatic fields. So in some cases where the hydrophobicity contributes a lot to ligand binding, the addition of the hydrophobic field may be critical to grasp the underlying relationship between structure and biological activity.

The best 3D-QSAR is derived from using all five fields afforded by CoMSIA (Table 2), which possesses the best predictive power ($q^2 = 0.691$). From the comparison of those several PLS analysis results of different fields in Table 3, it is likely that the properties considered intercorrelated in a complicated way. The intercorrelations of those numerically intensive grid fields are difficult to detect, so sometimes, it is relatively very difficult to determine whether some kind of field is more important or not. The advantages of using five different fields of well defined molecular properties has to be seen in the straightforward partitioning of these properties into spatial locations where they take a determining role on biological activity.
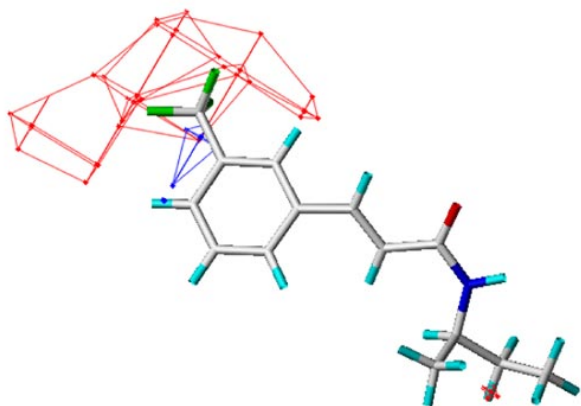
Figure 4 *The contour plots of the CoMSIA electrostatic fields (stdev*coeff). The favorable electrostatic areas with positive charges are indicated by blue isopleths, whereas the favorable electrostatic areas with negative charges are shown by red isopleths. The most active compound (27) is shown as the reference compound*
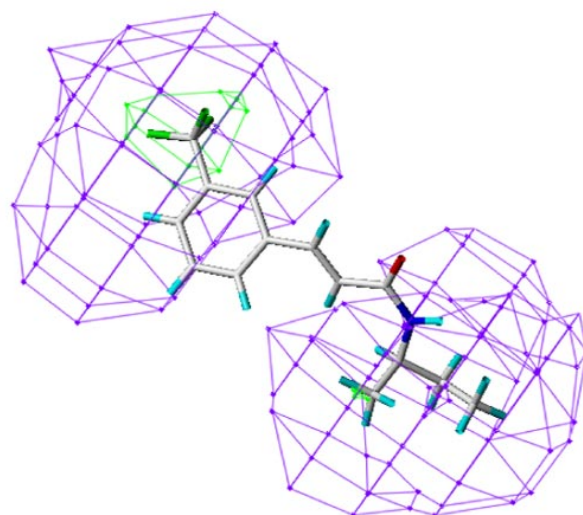

Figure 5 *The contour plots of the CoMSIA steric fields (stdev*coeff). The favorable steric areas with more bulk are indicated by green isopleths, whereas the disfavored steric areas are shown by purple isopleths. The most active compound (27) is shown as the reference compound*

Graphical interpretation of the results

One of the best advantages of CoMSIA is that the effects of all kinds of properties contributing to bioactivity can be divided and viewed as 3D coefficient contour plots. The coefficient contour plots may be helpful to determine the important regions where any changes of some kind of property may affect the biological activity and identify the important features contributing to interactions between ligand and receptor in the active site.

The CoMSIA steric and electrostatic fields based on PLS analyses are represented as 3D contour plots in Figures 4 and 5. In the electrostatic contour map (Figure 4), positive charge can be moved closer to the regions of positive coefficients (blue) and negative charge can be moved closer to the regions of negative coefficients (red). A close inspection of the electrostatic contour plots reveals that for the tested molecules the negative charge is preferred. Three red regions near the benzene ring indicate that more negative charge group substituted at sites 2, 3 and 4 on the benzene ring will enhance the biological activity. Previous 2D-QSAR analysis has uncovered that substituents with electron withdrawing effect increase the anticonvulsant activity of cinnamamides significantly [7], which can be easily interpreted from the electrostatic contour map. As to the blue region near the benzene ring, more positive charge is preferred on the benzene ring. Strong charge withdrawing groups linked to the benzene ring will make the charge distributed on the benzene ring relatively positive, which is expressed by the blue region.

From the fraction of the fields, it can be seen that the steric field contributes less than the electrostatic field. Areas indicated by green contours correspond to regions where steric occupancy with bulky groups are preferred, and areas encompassed by purple isopleths should be sterically avoided.. For the benzene ring on one end (A region), there exist two neighboring contour areas: a favorable area near the group substituted at the site 3 on the benzene ring and a larger adjacent unfavorable area around the benzene ring. The contour map near the benzene ring affords us some useful informa-
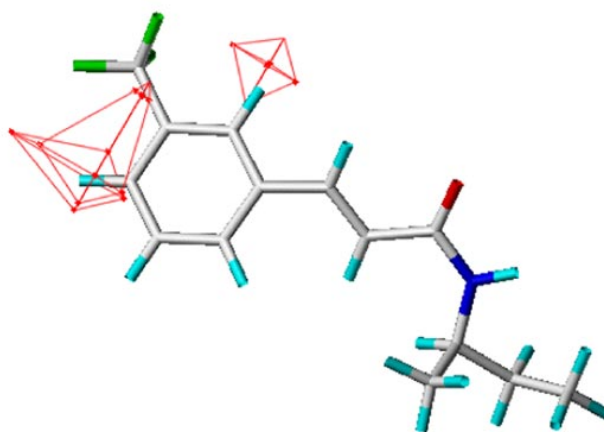

Figure 6 *The contour plots of the CoMSIA hydrophobic fields (stdev*coeff). The favorable hydrophobic areas are indicated by red isopleths, whereas the disfavored hydrophobic areas are shown by green isopleths. The most active compound (27) is shown as the reference compound*
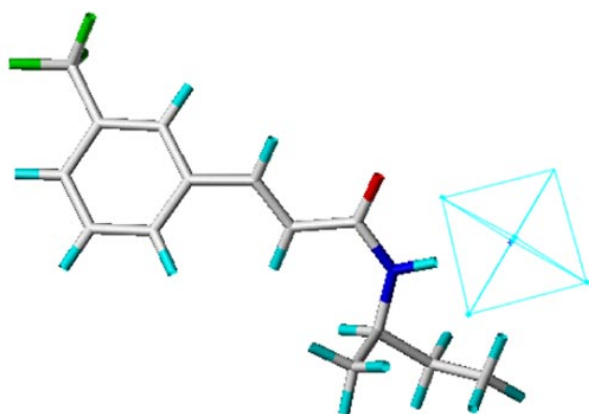
Figure 7 *The contour plots of the CoMSIA H-bond donor fields (stdev*coeff). Cyan isopleth contours maps beyond the ligands where an H-bond donor group in the ligand will be favorable for biological activity, while purple isopleths represents H-bond donor in the ligands unfavorable for biological activity. The most active compound (27) is shown as the reference compound*

Figure 8 *The contour plots of the CoMSIA H-bond acceptor fields (stdev*coeff). Magenta isopleth contours maps beyond the ligands where an H-bond acceptor group in the ligand will be favorable for biological activity, while red isopleths represents H-bond donor in the ligands unfavorable for biological activity. The most active compound (27) is shown as the reference compound.*
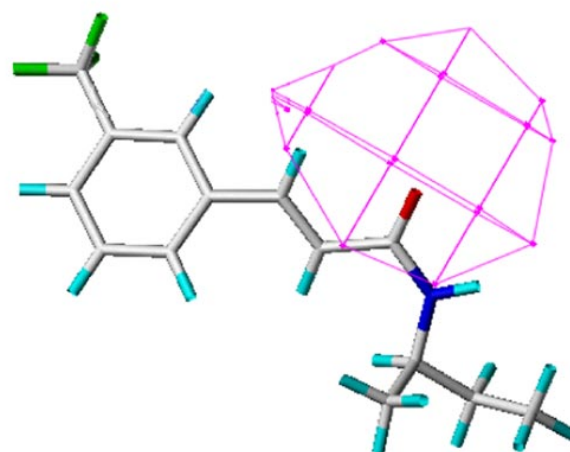
tion between inhibitors and receptor in terms of steric complementarity. When the inhibitors interact with its receptor, if the volume of some parts of the inhibitor increase, the contact area between the inhibitor and the receptor might become larger. However, when the contact area increases to a certain value, the steric complementarity will not be improved and even be depressed by the steric hindrance. So the groups substituted at the site 3 (sometimes site 4) on the benzene ring are sterically preferred to produce good steric and hydrophobic interactions (see hydrophobic contour map in Figure 6) with the receptor, but these bulky groups must be restricted to some extent in order to avoid bad steric contacts between the inhibitor and the receptor. Another sterically unfavorable site shown in Figure 5 is located near the substituents linked to the amido group (C region), and small substituents on this site will enhance the anticonvulsant activity.

The contour map of hydrophobic properties indicates two distinct hydrophobically favorable sites (Figure 6): one larger region near the substituents linked to the sites 3 and 4 on the benzene ring and the other one near the site 2 on the benzene ring, which means that groups with high hydrophobicity will favor biological activity. So it can be reasonably presumed that the benzene ring combined with these substituents on it are composed of a large hydrophobic core, and will produce a strong hydrophobic interaction with the receptor. In our previous work, the partition coefficient of the substituents on the benzene ring was determined to contribute significantly to biological activity [7], which is consistent with the results from the hydrophobic contour map. Moreover, the hydrophobic contacts between ligand and receptor should be suitably

orientated, which can be investigated by some tested compounds. For example, compounds 10, 11 and 12 have the same substituted group on benzene ring linked to different sites, but their biological activities are quite different. The reason is the CF_3 substituted on the different sites on the benzene ring, and CF_3 linked to sites 3 or 4 of compounds 10 or 12 have more suitable orientation then that linked to site 2 of compound 11, and consequently produce more favorable hydrophobic contacts with the receptor.

The graphical interpretations of the field contributions of the H-bond properties are shown in Figure 7 (H-bond donor field) and Figure 8 (H-bond acceptor field). In principle, they should highlight the areas beyond the ligands where putative hydrogen partners in the enzyme can form H-bonds that influence binding affinity. In Figure 7, the region near the hydrogen atom linked to nitrogen atom in amido group represented with cyan areas, is indicated as favorable H-bond donor site. In fact, this hydrogen atom is frequently involved as H-bond donor in hydrogen bonding. In the H-bond acceptor field (Figure 8), the favorable areas represent with the magenta isopleth are around the oxygen atom in amido group, which may be induced by the lone pair electron on oxygen atom in amido group. In a previous study, it had been assumed that the amido group might be an important part interacting with receptor, but its interaction mechanism was not clear [17]. From this analysis, it seems that the amido group can produce a strong H-bond with receptor, and the strength of the H-bonding can be greatly affected by the substituents linked to benzene ring through conjugating effects and the overall structure of the molecule.

Conclusions

In this study, the CoMSIA approach has been applied to correlate the anticonvulsant activity with the steric, electrostatic, hydrophobic and H-bonding fields of a set of cinnamimide analogues. By using five types of fields provided by CoMSIA, a 3D-QSAR model has been constructed. The derived model possesses promising predictive ability as indicated by the high cross-validated correlation and the prediction on the external test set, which is significantly superior to the model constructed by conventional CoMFA. Some important factors contributing to the biological activity can be reflected by the contour maps of different properties. The electrostatic and hydrophobic properties of the X group (Chart 2) will remarkably affect the biological activity, and highly electron-withdrawing and hydrophobic groups will enhance the biological activity, while these substituted groups must meet some steric restrictions. Large R groups in C region will be unfavorable to biological activity, meanwhile, the H-bonding of the amido group (B region) is essential for biological activity, which is directly related to the energetic complementarity between ligand and receptor.

The characteristics of the CoMSIA 3D contour plots derived in this study are very helpful for us to understand the underlying mechanism of receptor-drug interaction. This study in combination with our previously published QSAR studies of the cinnamamide derivatives are expected to provide rational information for designing new potential drugs.

Supplementary material available The 3D structures of all the molecules used in this paper are saved in PDB format.

References

1. Moffet, R. B. *J. Med. Chem.* **1964**, *7*, 319-325.

2. Van Heyningen, E.; Brown, C. N. *J. Med. Chem.* **1966**, *6*, 675-681.

3. Wang, Y. S.; Li, R. L.; Liu, W. Q.; Wang, G. Q.; Liu, P.; Xong, J. M.; Pei, Y. Q.; Yao, H.; Gao, X. M. *Acta Pharmaceutica Sinica* **1986**, *21*, 542-545.

4. Pi, Y. Q. *J. Chin. Med.* **1978**, *58*, 216-221.

5. Zhang, X. H.; Li, R. L.; Cai, M. S. *Beijing Medical College Transaction* **1980**, *12(2)*, 83-91.

6. Wang, Y. S.; Li, R.L.; Liu, W. Q.; Xu, X. J.; Guan Y. *Chin. Org. Chem.* **1986**, *8*, 217-220.

7. Hou, T. J.; Wang, J. M.; Liao, N.; Xu, X. J. *J. Chem. Inf. Comp. Sci.* **1999**, *39*, 775-781.

8. Cramer, R. D.; Patterson, D. E.; Bunce, J. D. *J. Am. Chem. Soc.* **1988**, *110*, 5959-5967.

9. Klebe, G.; Abraham, U.; Mietzner, T. *J. Med. Chem.* **1994**, *37*, 4130-4146.

10. Klebe G.; Abraham, U. *J. Comput. Aid. Mol. Des.* **1999**, *13*, 1-10.

11. Bohm, M.; Sturzebecher, J.; Klebe, G. *J. Med. Chem.* **1999**, *42*, 458-477.

12. Li, R.L; Wang, Y.S. *Acta. Pharm.* **1986**, *21*, 580-585.

13. SYBYL, version 6.5; Tripos Associates: St. Louis, MO, USA, 1999; http://www.tripos.com/.

14. Halgren, T. A. *J. Comput. Chem.* **1996**, *17*, 490-519.

15. Dewar, M. J. S.; Zoebisch, E. G.; Healy, E. F.; Stewart, J. J .P. *J. Am. Chem. Soc.* **1985**, *107*, 3902-3909.

16. Mopac, version 7.0; QCPE 688; Quantum Chemistry Program Exchange: Bloomington, USA, 1995; http://qcpe.chem.indiana.edu/.

17. Wang, Y. S.; Zhuo, J. C. *Beijing Medical College Transaction* **1982**, *14(1)*, 65-70.